J. Iran. Chem. Soc., Vol. 7, Suppl., July 2010, pp. S59-S69.

JOURNAL OF THE
Iranian
Chemical Society

High Efficiency ZnO Nano Sensor, Fabrication and Characterization

M. Hussain[a], M. Mazhar[a,*], T. Hussain[b] and N.A. Khan[c]
[a]Department of Chemistry/ [b]National Centre for Physics/ [c] Department of Physics, Quaid-i-Azam University, Islamabad-45320, Pakistan

(Received 18 November 2008, Accepted 24 July 2009)

Ultra fine thin films of pure and SnO doped ZnO nanosensor were grown on gold digitated ceramic substrate from bis(2, 4-pentanedionate)dimethylethanolamine zinc (II) using bis(2, 4-pentanedionate) tin(II) chloride as a dopant by ultrasonic aerosol assisted chemical vapor deposition technique (UAACVD) at temperature range of 400–450 °C under oxygen atmosphere at 5 Pa pressure. The sensitivity, selectivity, fast recovery, and reliability test performed on nanosensor suggested that both doped and undoped ZnO thin films are suitable for detecting ethanol vapor in the temperature range of at 60 to 150 °C, whereas at room temperature (25 °C) response and recovery time of the sensor increases many folds compared to 60 °C. Sensitivity of the ZnO sensor shows linear relationship with the increase of gas concentration. Electrical properties show that 1 % SnO doped ZnO enhanced the sensitivity of the film drastically and thus improved its detecting efficiency. Physico-chemical techniques like, CHNS-O, atomic absorption analyzer, and infra red and multinuclear nuclear magnetic resonance spectrometers were used for precursor characterization. X-ray diffractometer, scanning electron microscope, sigma scan analyzer and energy dispersive x-ray techniques were used for thin film characterization.

Keywords: Zinc oxide sensor, Doping, Synthesis, Ethanol

INTRODUCTION

Chemical sensor research is focused on producing efficient devices to sense the inflammable and hazardous vapors before they cross the threshold limits. Pure and doped ZnO is one of the first suitable semiconductors widely used for sensing O_2 [1], H_2 [2], NO_x [3-5], ethanol [6-10] and humidity [11], which shows instant change in electrical resistance when exposed to inflammable materials like organic solvent vapors, petrol vapors and methane gas that pose a threat to safety when they cross their thresholds limit in air. Most of research work deals with pure and doped ZnO thin film by rare earth atoms [11-20], and transition elements [21] encourage their use as gas sensing devices [22], transparent electrodes [23] and piezoelectric devices [24]. Gas sensing properties in n-type ZnO thin film is achieved by decrease in electrical resistivity in response to increasing amount of reduced gases in air. The reason for decrease in resistivity can be explained by absorption of oxygen on the surface and grain boundaries of metal oxide at high temperatures. Film type sensor can be fabricated with various techniques such as spray pyrolysis, sputtering, laser ablation, sol-gel method and chemical vapor deposition [25,26]. In this work, a high efficiency gas sensing device has been modeled, designed, fabricated using ultrasonic aerosol assisted chemical vapor deposition technique and tested for ethanol vapor sensing. X-ray diffraction (XRD), scanning electron microscopy (SEM) and resistance measurement are used to characterize the microstructure and

*Corresponding author. E-mail: mazhar42pk@yahoo.com

electrical properties of the doped and undoped ZnO gas sensor film that were deposited on ceramic substrate.

EXPERIMENTAL

Materials and Methods

Analytical grade reagents 2-methoxyethanol, tin(II) chloride and N,N-dimethyl ethanolamine (dmeaH), purchased from Sigma/Aldrich were used for the synthesis of the precursor without further purification. All other chemicals were purchased from Merck and were used as supplied. All syntheses were performed in air ambient using a 20 KHz ultrasonic generator. Melting points were measured with a GallenKamp 3A-3790 and are uncorrected. Elemental analyses (CHNO) were performed by a CHNS-O Flash EA 1112 of Thermoelectron instrument. Analysis for Zn was carried on an atomic absorption spectrometer, model GBC 902. FTIR (model Nexus 470 FTIR), NMR (Avance 300 MHz, BRUKER) and single crystal x-ray diffractometer (Bruker, AXS SMART APEX CCD) were used to identify molecular structure of the precursor. Thermal studies and decomposition patterns were studied using a TGA/SDAT 851^e Mettler Tolledo coupled with FTIR Nexus 470 of Thermo Nicolet. Sigma scan analyzer (Stylo, USA) was used for the measurement of film thickness. Powder X-ray diffraction studies were performed using a powder X-ray diffractometer (PAN Analytical X' Pert PRO) equipped with a Cu source (Cu $K_{\alpha,}$ λ = 1.5405 Å). SEM and EDX (JOEL-JSM-5910) were used to determine surface morphology, average particle size and composition of the deposited thin film material. The electrical properties of the oxide film under various conditions were measured by a self-designed improved two-probe set up as previously reported [27]. All electrical contacts were gold plated to minimize the resistance due to the system.

Syntheses

Bis (2,4-pentanedionate)dimethylethanolamine zinc(II) (1). 2.81 g (0.01 mol) bis(2,4-pentanedionate) zinc(II) mono hydrate, 2.0 g (0.02 mol) of dimethylethanolamine (dmeaH) and 15 g of methanol and 7 g of acetonitrile were mixed in a 250 ml Erlenmeyer flask. The flask was covered with a polythene film and then placed in an ultrasonic generator at a temperature of 40 °C for 2-3 h to produce a concentrated clear solution. The concentrated contents were taken out of the ultrasonic bath and set aside at room temperature for crystallization. The crude white brittle product bis(2,4-pentanedionate)dimethylethanolamine zinc(II) obtained was dissolved in 1:1 toluene and diethyl ether mixture and placed for recrystallization at room temperature under slow evaporation. Crystals were recovered by filtration, washed with diethyl ether and dried in air (m.p.130 °C). The yield was 90 %. The molecular structure was confirmed by single crystal x-ray analysis. Elemental analysis found C, 47.93; H, 6.91; O, 23.1; N, 3.65, 18.78 Zn %. Calcd. for $C_{14}H_{25}O_5NZn$: C, 47.67; H, 7.09; O, 22.7; N, 3.97; Zn, 18.56%. FTIR (cm^{-1}), 3268, 3213, 2998, 2965, 2915, 2833, 1600, 1509, 1459, 1393, 1318, 1252, 1194, 1086, 1052, 1012, 946, 913, 888, 755, 656, 540. ^{1}H NMR, NMR 300 MHz, (C_6D_6, ppm): δ 1.933 [singlet 12 H, CH_3 –C] , δ 2.243 [singlet 6 H $(CH_3)_2$–N] , δ 2.399-2.434 [multiplet 2H NCH_2 -CH_2 –], δ 3.785-3.818 [multiplet 2 H, OCH_2 -CH_2 –], δ 5.288 [singlet 2H, *H* - C $(C)_2$], C^{13} NMR (300 MHz, C_6D_6: δ 27.52 $(\mathbf{C}H_3)_2$–CH, δ 45.21 $(CH_3)_2$–N, δ 57.44 $(\mathbf{C}H_3)_2$–N-CH_2 , δ 60.73 OH-CH_2, δ 99.47 O=C-$\mathbf{C}H_3$, δ 191.79 HO-CH_2- $\mathbf{C}H_2$.

bis(2,4-pentanedionate) tin(II) chloride (2). 1.90 g (0.01 mol) anhydrous tin(II) chloride, 5 g (0.025 mol) of acetylacetone and 10 g of 2-methoxy ethanol were mixed in a 250 ml Erlenmeyer flask. The flask was covered with a polythene film and then placed in an ultrasonic generator at a temperature of 40 °C for 2-3 h to produce a concentrated clear solution. The contents were taken out of the ultrasonic bath and placed in freezer for crystallization. White block crystals of bis(2,4-pentanedionate) tin(II) chloride were obtained in 90 % yield (m.p. 198 °C) after 12 h. The crystals were isolated through filtration, washed with petroleum ether and dried in air. The molecular structure was confirmed by single crystal x-ray analysis. Elemental analysis found C, 35.75; H, 3.89; O, 9.03; Sn 34.01 %. Calcd. for $C_{10}H_{14}O_2$ $SnCl_2$: C, 35.11; H, 3.93; O, 8.99; Sn, 33.34 %. FTIR (cm^{-1}), 3318, 3268, 2940, 2880, 1580, 1509, 1397, 1351, 1308, 1245, 1197, 1144, 1245, 1197, 1116, 1073, 1052, 917, 865, 849, 770, and 650 cm^{-1}. ^{1}H NMR 300 MHz, ($CDCl_3$, ppm): 1.85 (singlet, 6H, CH_3), 5.71 (singlet, 1H, C*H*); ^{13}C NMR ($CDCl_3$, ppm): 27.99 (CH_3), 49.21 (CH), 196.12 (C=O).

Table 1. Growth condition for the deposition of undoped and doped metal oxide thin film from *bis* (2,4-pentanedionate) (dimethylethanolamine) zinc (II).

Precursor concentration.	200 mg/25 ml (methanol)
Carrier Gas (O_2) pressure (Pa)	5
Sample solution injection (ml/min).	0.5
Substrate.	quartz, ceramic, stainless steel.
Substrate Temperature.	400-450 °C
Deposition time.	10-30 min (depending upon thicknes

Thermal Decomposition Study

Thermal behavior of bis(2,4-pentanedionate)dimethylethanolamine zinc(II) was studied in the range of 30 – 500 °C with a heating rate of 5 °C min^{-1} under an O_2 atmosphere in an open lid 70 µL alumina crucible. For mechanistic studies, precursor samples were heated at 160 °C and 360 °C, the temperatures where maximum weight loss occurred. The residual masses recovered at this temperature were subjected to FTIR studies to get information about the sequence of decomposition.

Thin Film Deposition

The thin film deposition apparatus was described previously in detail [26]. The conditions used for the growth of the ZnO thin films are given in Table 1. 200 mg of bis(2,4-pentanedionate)dimethylethanolamine zinc(II) in 25 ml methanol was injected into an Ultrasonic Atomizer (Cole Palmer) to generate the aerosol in an evacuated quartz chamber containing 50 × 40 mm ceramic wafers inter digitated with gold pattern prepared by using standard PCB technique. The ceramic wafer was cleaned with deionized water, acetone and 1,1,1- trichloroethane and then heated to 100 °C for twenty minutes before use. Oxygen gas and sample solution was injected through a control valve.

Gas Sensing Studies

The deposited thin film was placed in self designed apparatus as shown in Fig. 1. H-bulb with thermostatic control was placed under the substrate for control of heating and the corresponding temperatures were measured using a thermocouple and digital thermometer attached to the substrate support. Electrical resistance was measured with the help of a digital multimeter attached via a computerized control system to the sensor. This records the resistance every one second. The electrical resistance was measured for each SnO doped and undoped ZnO film against temperature in relation to ethanol vapors (G) to the resistance in air (Ga) at respective temperature for a fixed ethanol volume (500 ppm)

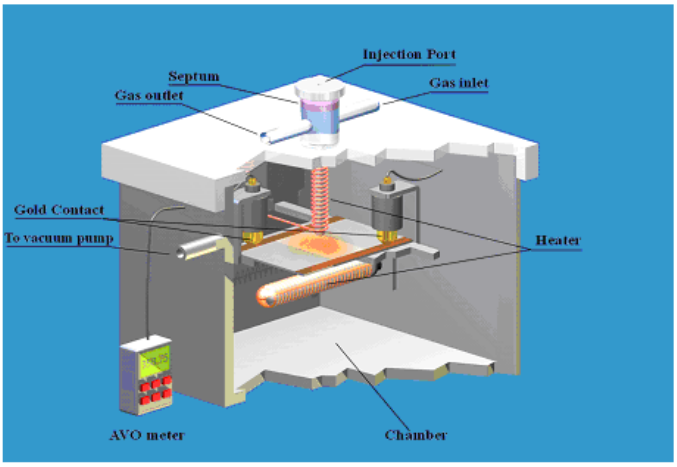

Fig. 1. Pictorial view of assembly used to study gas sensing property of ZnO film.

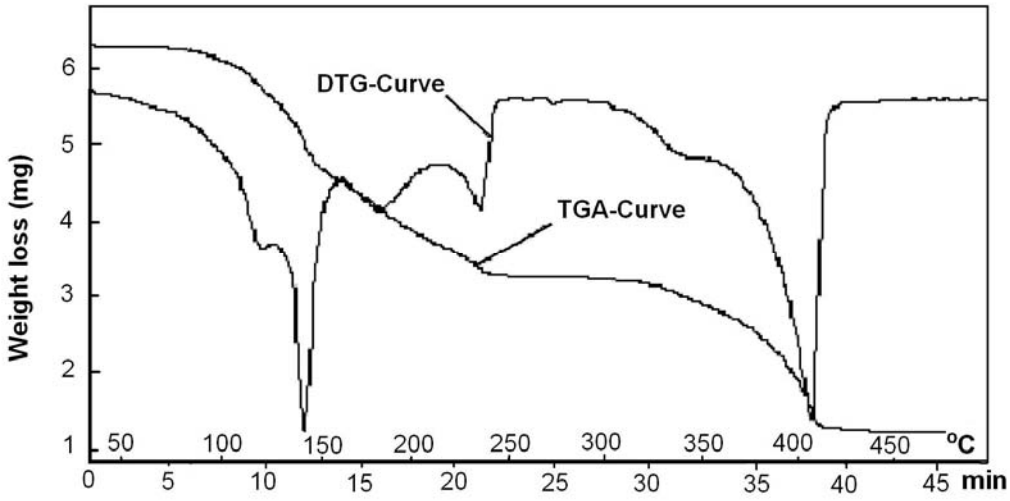

Fig. 2. TGA/DTG curves showing decomposition of Zn $(acac)_2$ dmaeH.

sprayed on thin film after passing through thermostatic hot tube kept at a temperature of 150 °C to avoid condensation. The sensitivity, S, was calculated as the ratio of Ga/G [28]. The change in electrical resistance was also determined for ethanol vapor concentration from 50 to 2000 ppm at a temperature of 60 °C.

RESULTS AND DISCUSSION

Ceramic semiconductors such as ZnO and SnO with nanoparticle size show high response to electrical conductivity when exposed to trace amount of hydrocarbon based gases, such as CH_4 at high temperature. Doped and undoped ZnO semiconductors are extensively used to sense toxic gases before they cross permitted limits. There are several methods e.g., sol-gel, CBD, CVD, sputtering, available for fabrication of doped/ or undoped ZnO nanosensors. We developed a chemical method in which bis(2,4-pentanedionate)dimethylethanolamine zinc(II) is used as a precursor for the fabrication of ZnO and SnO doped ZnO nanosensor via UAACVD. Both the precursor and dopant are readily prepared by a simple chemical mixing of reactants in appropriate solvent under ultrasonic irradiation as shown in chemical reactions 1 and 2.

$$Zn(acac)_2 + dmaeH \xrightarrow[\text{methanol+acetonitrile}]{)))))))} Zn(acac)_2\ dmaeH \quad (1)$$

$$\left[acac = CH_3COCOCH_3,\ \ dmaeH = (CH_3)_2NCH_2CH_2OH \right]$$

$$2acacH + SnCl_2 \xrightarrow[\text{2-methoxyethanol}]{)))))))} Sn(acac)_2Cl_2 + H_2 \quad (2)$$

Sonochemical synthetic route adopted for both the complexes is simple and gives high yield as compared to the previously reported methods [29,30].

All the characteristic IR vibrational frequencies have been assigned and are in agreement with the proposed molecular structure. The O-H stretching frequencies were found at 3268-3213 cm^{-1}, and C-N stretching at 1252-1194 cm^{-1} indicating the presence of ethanolamine. Also the symmetric and antisymmetric CH_3 vibrations observed around 2965 cm^{-1} and 2833 cm^{-1} confirmed the presence of the methyl group attached to nitrogen. The absorption band at 1459 cm^{-1} is due to the in plane bending vibration of CH_2 group and bands at 1393-1318 cm^{-1} indicates the symmetric vibrations of CH_3 group attached to nitrogen atom. The bands at 913 cm^{-1} and 656 cm^{-1} are due to vibration of M-N and M-O bonds, respectively.

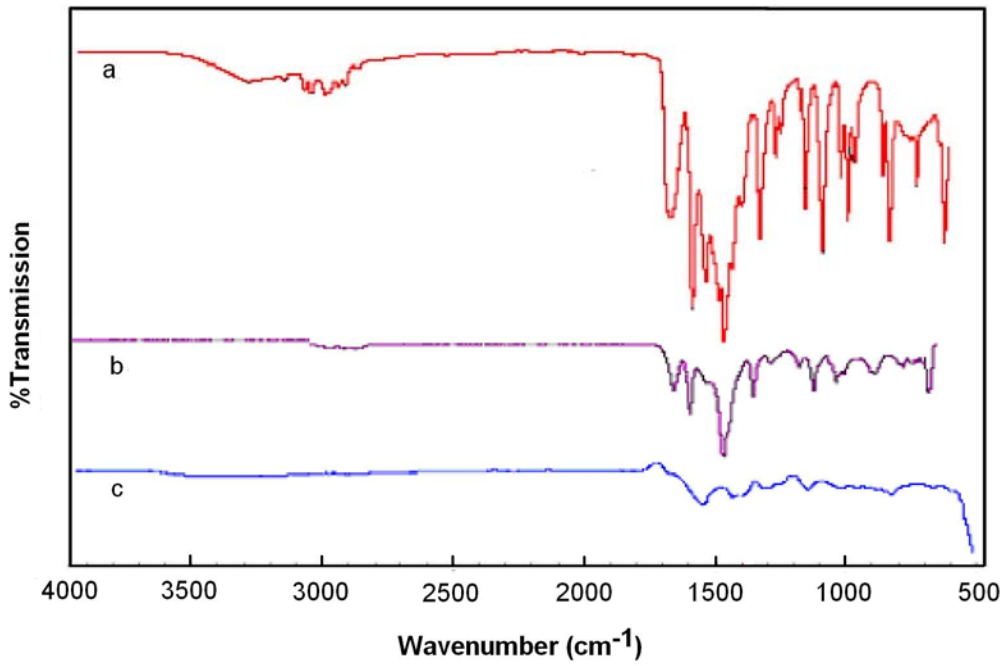

Fig. 3. FTIR spectrum of a) Zn $(acac)_2$ dmaeH complex recorded at room temperature, b & c) spectrum of residual masses after heating at 160 °C and 360 °C.

Thermal Decomposition Study

The TGA and DTG curves of $Zn(acac)_2$ dmeaH (Fig. 2) show that decomposition of the complex is complete at 410 °C with a residual mass of 19.2 %, a value consistent to the formation of ZnO as being the final product. The complex shows three weight losses. The first weight loss of 24.48% is due to loss of dmeaH. This was confirmed from the FTIR spectrum of residual mass obtained after heating the complex at 160 °C which shows absence of characteristics dmeaH peaks and leaving behind $Zn(acac)_2$ as a residual mass (Fig. 3, spectrum b). The second and third weight losses are 26.79% and 32.1% and in total come to 58.89% (calcd. total of 56.7 % for acac) that are assigned to loss of two acac groups. A little increase of loss in weight i.e., 2.19% from the calculated weight loss of 56.7% for two acac groups is due to sublimation characteristics of residual zinc acetylacetonate. This sublimation characteristics is an added advantages to use such precursors in CVD technique for the deposition of smooth thin films of metal/or metal oxide. The removal of acacH and leaving ZnO as residue would take place via hydrogen abstraction. This observation is confirmed by seeing the residual FTIR spectrum, which shows elimination of typical acac peaks (Fig. 3, spectrum c). On the basis of the above observations and thermal decomposition studies of metal acetylacetonates, a decomposition mechanism for $Zn(acac)_2$ dmeaH is suggested as below.

$$Zn(acac)_2.dmeaH \xrightarrow{160^\circ C} Zn(acac)_2 \downarrow + \ dmeaH\uparrow$$

$$Zn(acac)_2 \xrightarrow[6O_2]{260\ ^oC} acacH \downarrow + 2CO_2 \uparrow + CH_3COCH_3 \uparrow + ZnO\downarrow$$

$$3acacH \xrightarrow[2O_2]{>360\ ^oC} 4CH_3COCH_3 \uparrow + 3CO_2 \uparrow$$

The proposed decomposition pattern of $Zn(acac)_2$ match with the previous studies [31].

XRD Study

The grain size of undoped and SnO doped ZnO thin film was determined using Debye-Scherrer equation [32]. Peak intensities, d-spacing, 2θ values and integral breadth of the

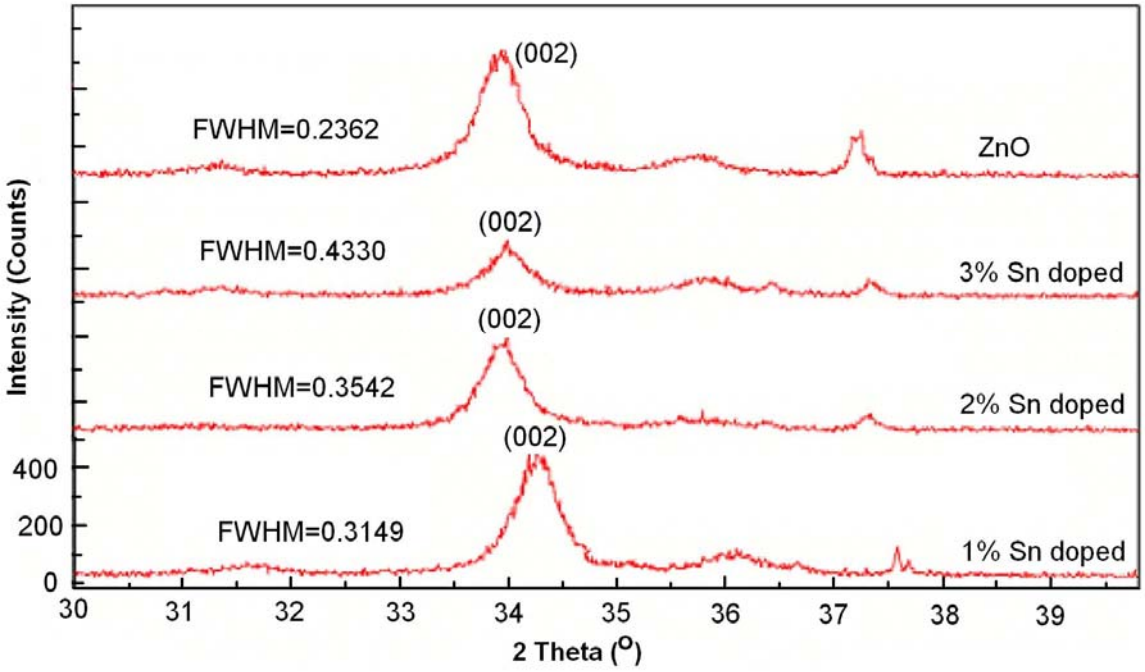

Fig. 4. XRD spectrum of doped and undoped ZnO thin film.

reflections were determined with X'Pert Data Collector software.

The average grain size as calculated was found in the range of 25 ± 10 nm. The calculated grain size agrees with the results obtained by SEM. The x-ray diffraction data confirmed that the film coated on ceramic substrate has only c-axis orientation (002) plane and wurtzite structure of ZnO thin films. The results are in agreement with the previous study [33]. This was due to the lowest surface free energy [32] of the most densely packed (002) plane in wurtzite ZnO structure.

XRD patterns (Fig. 4) also revealed that all the deposited films were crystalline and retain wurtzite structure. Moreover the intensity of (002) peaks gradually decreased and broadened according to increase in SnO dopant. With increasing dopant concentration, the location of (002) plane in terms of diffraction angle does not change significantly. However, in case of 1 % Sn dopant, the peak position of the (002) plane was shifted to higher 2θ value, which ultimately resulted in decrease of the crystallite size. The reason is that the lattice parameters of SnO:ZnO was decreased in the c-axis with 1% SnO dopant. As a result, the full width at half maximum (FWHM) of the 002 peaks decrease by a factor of 0.2 °. Another reason would be at lower concentration of doped SnO (1% or less) in which the incorporation of dopant would take place only at substitutional sites of zinc and has profound effects on structural properties of ZnO thin film. However, for higher dopant concentration (> 1%), one would expect that due to the incorporation of SnO into ZnO lattice, the dopant is unable to induce a considerable change in structural properties of the ZnO thin film.

It can be concluded from the above discussions that the ultrasonic aerosol assisted chemical vapor deposition technique does have significant effects on crystallinity enhancement, and the strong preferential orientation along (002) plane as illustrated in Fig. 4. However, for ZnO film deposited by the traditional SILAR procedure without the ultrasonic irradiation, only weak crystallinity degree and orientation growth along the c-axis were obtained as reported previously [34-36].

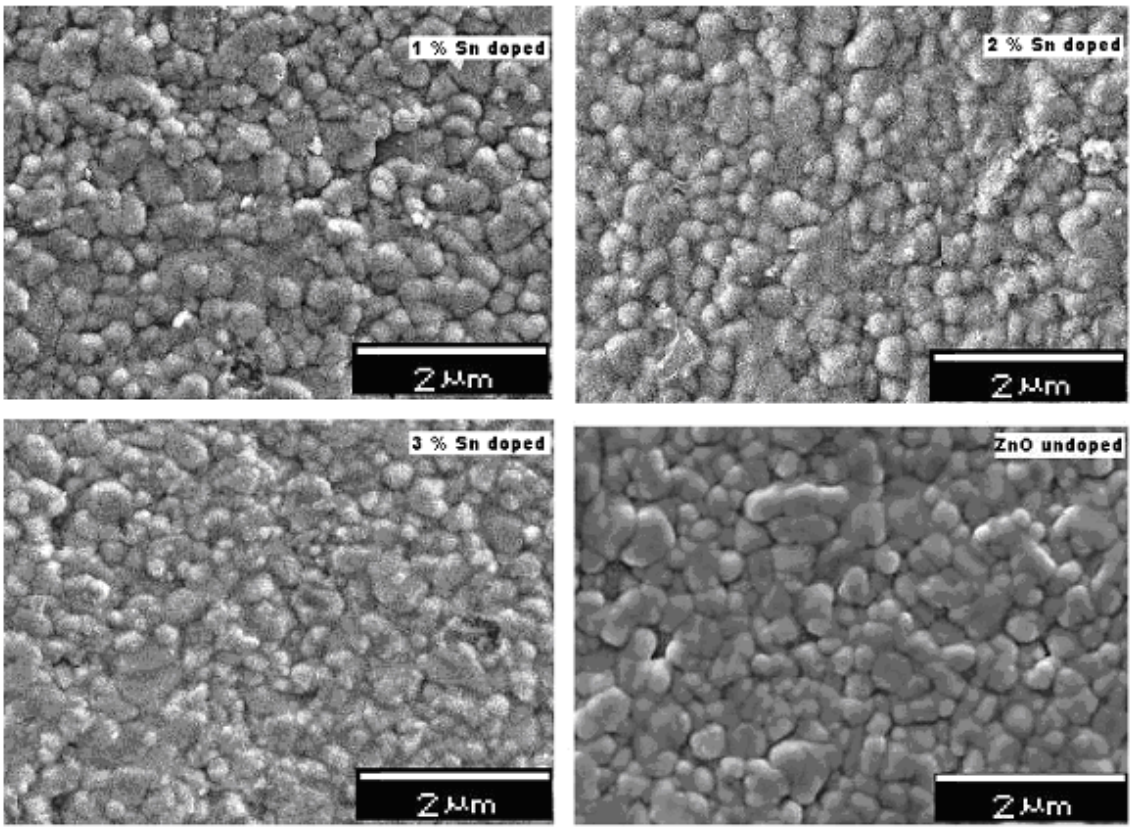

Fig. 5. SEM images of SnO doped and pure ZnO thin film

SEM Study

The SEM images of the tin doped and undoped ZnO films indicate their granular character. The average grain size measured from these images was in the range of 30 ±10 nm. The micro structural images (Fig. 5) taken for all doped and undoped samples revealed that the grain size in general was smaller for the tin oxide doped than the undoped samples. These images also revealed that the doped films were denser and have more spherical grains than the undoped film.

Ethanol Sensing

It is reasonable to believe that in n-type semiconductors like ZnO thin film, oxygen atoms from the gas phase, remove localized mobile electrons from the surface of the grain of ZnO thin film and become adsorbed as negative ions [37,38]. This leads to the formation of an electron-depleted surface, which changes the electrical conductivity of the semiconductor and ultimately reduces the height of the barrier. This can be represented as $O_2 + 2e^- \rightarrow 2O^-$ or $2O_2 + 2e^- \rightarrow 2O_2^-$. This charged oxygen species can act as electron donors when exposed to reducing gases. When the proposed gas sensor is exposed to ethanol vapors, the initial adsorption of ethanol on the surface of the ZnO displaces the charged oxygen (O^-, O_2^-) and causes the oxygen to depart as O_2 leaving the ejected electron from the (O^-, O_2^-) into the depleted area of ZnO. Because of these injected electron from the displaced oxygen, the resistance of the sensor decreases. This decrease of the resistance mainly depends on temperature and gas concentration. In general there exist an optimum operating temperature and gas concentration at which the mechanisms of

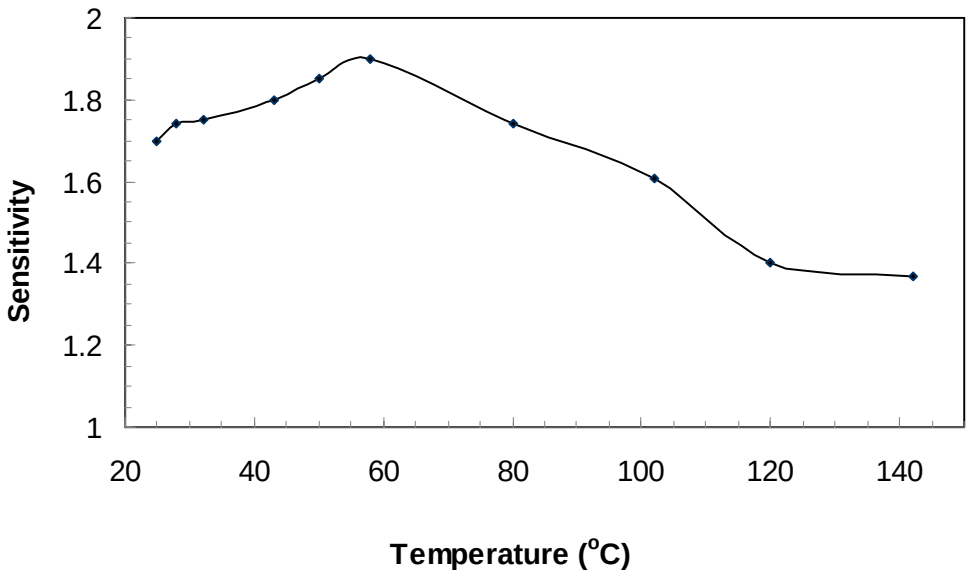

Fig. 6. Sensitivity of ZnO thin film at various temperatures for a fixed concentration of ethanol vapors (500 ppm).

desorption and dissociation of a gas on the particular surface can achieve the maximum sensitivity. Now considering these types of effects, the resistance of a gas sensor in the presence of air is expected to be high because there is a large number of oxygen ion species (O^-, O_2^-) on the surface that have drawn electrons from the underlying metal oxide leaving large number of electron depleted hole and ultimately increase the resistance. Our results showed the maximum sensitivity for detecting 500 ppm ethanol vapor, determined as Ga/G, where G and Ga are the resistances in the presence of 500 ppm ethanol and air respectively, was ~ 2 at 60 ºC, Fig. 6. The corresponding resistance and time showed the sensing characteristics in terms of sensitivity, response and recovery time, Figs. 7 and 8. The response time is defined as the time required to reach until 90 % of the response signal is reached, whereas recovery time denotes the time needed until 90 % of the original baseline signal is recovered. It is evident that the sensitivity value found is too low compared to the value of 20 to 180 depending upon concentration pulses of ethanol vapors for a fixed temperature of 400 ^oC reported previously [39], but its response and recovery times towards ethanol gas were about 10-15 s with good reproducibility. These are much better than the previous report [39] in which response and recovery time was about 2-4 min. Figs. 7 and 8 also show that after initial resistance was stabilized, the injected ethanol turns into vapor phase after passing through thermostatically controlled tube maintained at a temperature of 150 ^oC to avoid any condensation. These ethanol vapors strikes with the surface of ZnO thin film in the test chamber, as a result the resistance of the sensor decreases and soon after it becomes saturated. After few second when the ethanol vapors were removed due to evaporation, the resistance of the sensor increased. The reaction between ethanol and ionic oxygen species (O^-) takes place in two different ways as reported earlier [40].

The response and recovery time (time for approximately 90% resistance change) for ethanol vapor /air mixture for 500 ppm concentration at temperature of 60 ^oC is about 10-15 seconds with good reproducibility.

For a particular concentration of ethanol vapors, say 500 ppm, the sensitivity decreased almost 100% as the temperature was raised from 60 to 200 ^oC. These results are in contrary to the previous work [29], in which the sensitivity increases with increasing operating temperature. The incorporation of 1% SnO in ZnO thin films shows an improvement of electrical conductivity of bulk ZnO, which decreased with the increase of Sn dopant concentration.

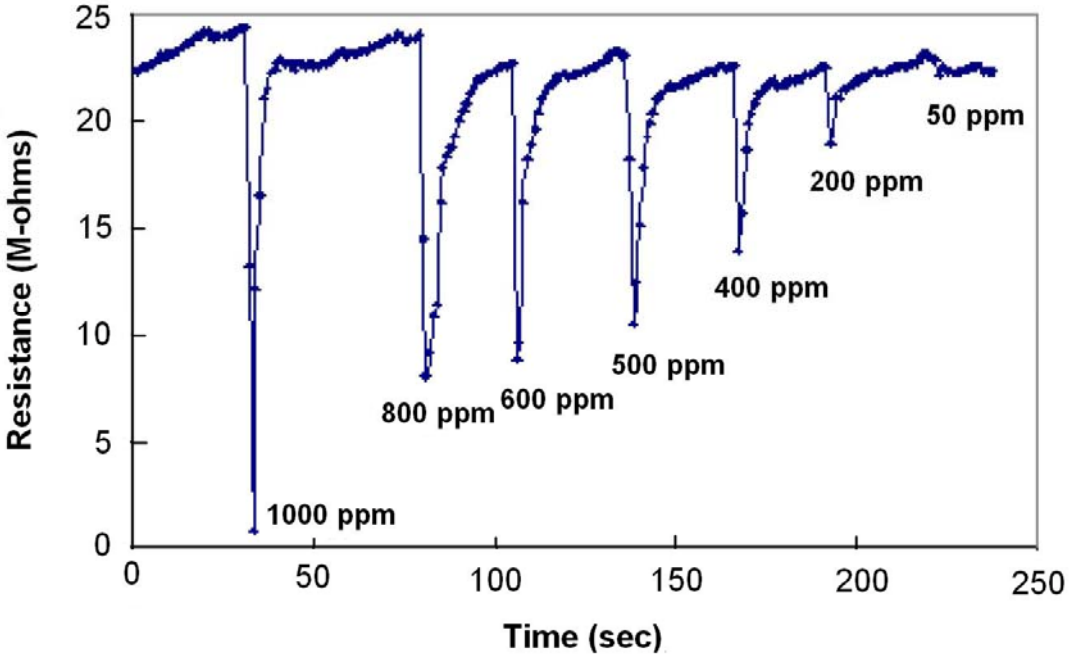

Fig. 7. Transient response characteristics as a function of ethanol concentration for ZnO thin film as operated at 60 ^{o}C.

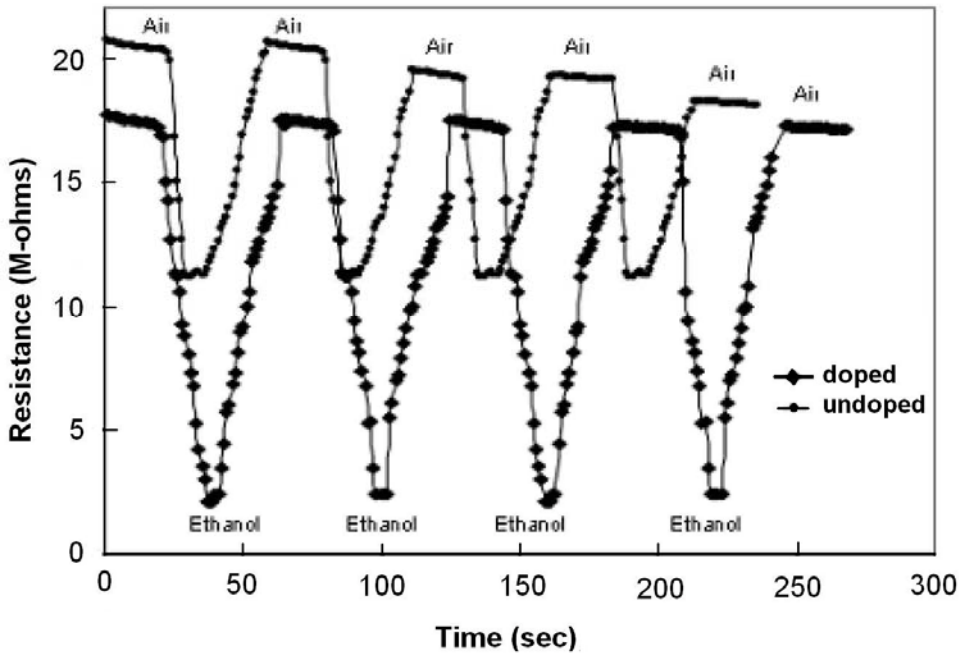

Fig. 8. Transient response characteristics of doped/undoped ZnO sensor at operating temperature of 60 ^{o}C.

CONCLUSIONS

Ultra fine ZnO thin films nanosensor of thickness < 2 μm has been successfully fabricated by UAACVD technique using $Zn(acac)_2$dmeaH and Sn $(acac)_2Cl_2$ complexes as precursors and dopant respectively onto ceramic substrate inter digitated with gold pattern plated and tested as ethanol gas sensor. The crystalline sizes of ZnO hexagonal particles as determined by XRD and SEM were found to be in the range of 25 ± 10 nm. The gas sensing performances of films were mainly investigated in the range of (50-2000 ppm) of ethanol with the operating temperature at 60°C. The sensors had n-type response to these vapors with response and recovery times within seconds. The sensor characteristics to reducing ethanol gas showed significantly dependence on gas concentration and temperature. The 1 % SnO as a dopant has strongly improved the sensor sensitivity and selectivity for sensing ethanol vapours which found to be maximum at 60 ^oC. A mechanism for the thermal decomposition of the precursor to targeted ZnO film has been presented.

ACKNOWLEDGEMENTS

The authors gratefully acknowledge help of IICS staff for assistance during the measurements and Pakistan Science Foundation for financial support.

REFERENCES

[1] G. Sberveglieri, S. Groppelli, P. Nelli, F. Quaranta, A. Valentini, L. Vasanelli, Sens. Actuators. B 7 (1992) 747-751.

[2] T. Yamazki, S. Wada, T. Noma, T. Suzuki, Sens. Actuators. B (1993) 14 594-595.

[3] J. Muller, S. Weissenrieder, Fres. J. Anal. Chem. 349 (1994) 380-384.

[4] C. Lingyuanb, B. Shoulia, Z. Guojuna, L. Dianqinga, C. Aifana, C. C. Liu, Sens. Actuators. B 134 (2008) 360-366.

[5] S. C. Nwall, V. Ravi, I. S. Mulla, S. W. Gosavi, S. K. Kalharmi, Sens. Actuators. B 126 (2007) 382-386.

[6] K. Stambolova, S. Konstantinov, P. Vassilev, Ts. Peshev, T. Sacheva, Lanthanum Mater. Chem. Phys, 63 (2000) 104-108.

[7] Y. J. Chen, C. L. Zhu, G. Xiao, Sens. Actuators. B 129 (2008) 639-642.

[8] Z. Yang, L. M. Li, Q. Wan, Q. H. Liu, T. H. Wang, Sens. Actuators. B 135 (2008) 57-60.

[9] B. P. J. De Lacy Costello, R. J. Ewen, N. Guernion, N. M. Ratcliffe, Sens. Actuators. B 87 (2002) 207-210.

[10] S. M. Chou, L. G. Teoh, W. H. Lai, Y. H. Su, M. H. Hon, Sensors. 6 (2006) 1420-1427.

[11] T. J. Hsueh, C. L. Hsub, S. J. Changa, I. C. Chen, Sens. Actuators. B 126 (2007) 473-477.

[12] J.A. Garcia, A. Remon, J. Piqueras, J. Appl. Phys. 62 (1987) 3058.

[13] Y. Bobitski, B. Kotlyarchuk, D. Popovych, V. Savchuk, Proc. SPIE. 4425 (2001) 342.

[14] O. Takai, M. Futsuhara, G. Shimizu, C. P. Lungu, J. Nozue, Thin Solid Films. 318 (1998) 17.

[15] R. Ondo-Ndong, G. Ferblantier, M. Al Kalfioui, A. Boyer, J. Cryst. Growth. 255 (2003) 130.

[16] J. H. Lee, K.H. Ko, B.O. Park, J. Cryst Growth. 247 (2003) 119.

[17] F. Demichelis, C. F. Pirri, E. Tresso, Proc. SPIE. 2253 (1994) 103.

[18] P. F. Carcia, R. S. McLean, M. H. Reilly, G. Nunes, J. Appl. Phys. Lett. 82 (2003) 1117.

[19] J.Wang, X. Wang, X. Jiang, S. Yang, D. Gao, G. Du, Proc. SPIE. 112 (2001) 4580.

[20] D. Zhang, Z.Y. Xue, Q. Wang, J. Ma, Proc. SPIE. 4918 (2002) 425.

[21] W. H. Zhang, W. D. Zhang, Sens. Actuators. B 134 (2008) 403-408.

[22] C. H. Kwon, H. K. Hong, D. H. Yun, K. Lee, S. T. Kim, H. Roh, Y. B. H. Lee, Sens. Actuators. B 24-25 (1995) 610.

[23] S. Major, S. Kumar, M. Bhatnagar, K.L. Chopra, J. Appl. Phys. Lett. 49 (1986) 394.

[24] M.G. Ambia, M.N. Islam, M. Obaidul Hakim, J. Mater. Sci. 27 (1992) 5169.

[25] O. Takai, M. Futshara, G. Shimizu, C.P. Lungu, J. Nozue, Thin Solid Films. 318 (1998) 117-119.

[26] M. Mazhar, S.M. Hussain, F. Rabbani, K.K Gabriele, K. C. Molloy. Bull. Kor. Chem. Soc. 27 (2006) 1572-1576.

[27] A.E. Jimnenz-Gonzailez, P.K. Nair, Semicond. Sci. Technol. 10 (1995) 277.

[28] K. Ihokura, J. Watson, "The stannic oxide Gas Sensor Principles and Applications" CRC Presss, Boca Raton, 1994, p.35.

[29] M. Hamid. M. Mazhar. A. Asif, M. Zeller, A. D. Hunter, Acta. Cryst. E61, (2005) 1539-1541.

[30] S. Shahzadia, S. Ali, G.-X. Jin, J. Iran. Chem. Soc. 3 (2006) 323-326.

[31] J. Von Hoene, R.G. Charles, W.M. Hickam, J. of Thermal Analysis and Calorimetry. 62 (1958) 1098-1101.

[32] X.D. Gao, X.M. Li, W.D. Yu, J. Inorg. Mater. 19 (2004) 610.

[33] V. E. Henrich, P. A. Cox. Appl. Surf. Sci. 72 (1993) 277.

[34] R. S. Morrison, Semiconductors sensors, ed. Sze, S. M. New York, John Wiley, 1994, p. 383.

[35] C. Liewhiran, S. Phanichphant, Sensors. 7 (2007) 650-675.

[36] G. Srinivasan, J. Kumar, Cryst. Res. Technol. 41 (2006) 893-896.

[37] Y.E. Lee, Y.J. Kim, H.J. Kim, J. Mater. Res. 13 (1998) 1260-1265.

[38] Y.F. Nicolau, Appl. Surf. Sci. 22/23 (1985) 1061.

[39] S. M. Chou, L. G. Teoh, W. H. Lai, Y. H. Su, M. H. Hon, Sensors. 6 (2006) 1420-1427.

[40] S. Mishra, et.al. Bull. Mater. Sci., 25 (2002) 231-234.